Search for Lepton Flavor Violation with Muons

Toshinori Mori

International Center for Elementary Particle Physics, the University of Tokyo
7-3-1 Hongo, Bunkyo-ku, Tokyo 113-0033, Japan

E-mail: mori@icepp.s.u-tokyo.ac.jp

ABSTRACT

Now that the neutrino oscillation phenomena have been established, any new physics scenario beyond the standard model necessarily involves lepton flavor violation (LFV) also in the charged lepton sector. Particularly TeV supersymmetry predicts large branching ratios for some of the LFV processes that may be accessible to coming experiments. Most promising LFV processes are the rare muon decays $\mu \to e\gamma$ and $\mu \to e$ conversion, which require quite different experimental approaches. The first of such LFV search experiments that are sensitive to new physics, is the MEG experiment. It aims to discover $\mu \to e\gamma$ with at least two orders of magnitude higher sensitivity than previous experiments. It might lead to first clear evidence of new physics, likely to be supersymmetry, just before LHC start-up. Experiments looking for $\mu \to e$ conversion, MECO, and PRISM/PRIME later, are also being prepared.

1. Lepton Flavor Violation in Charged Leptons

Physics motivation for lepton flavor violation (LFV) in charged leptons, in a simple-minded experimentalist's view, is summarized in Fig. 1.

In a mysterious three generation structure, quarks mix each other, neutrinos oscillate into each other, then charged leptons must be destined to mix each other too. The only question is how much they mix, or more adequately, whether their mixings are within our experimental reach.

Supersymmetric grand unification theories (SUSY GUTs) beautifully unify three forces at extremely high energy of 10^{16} GeV. SUSY GUTs also unify quarks and leptons and thus relate quark mixings to charged lepton mixings at the GUT scale. Thanks to the heavy top quark, SUSY GUTs predict the branching ratio of muon's LFV decays $\mu \to e\gamma$, for example, as large as the current experimental limit [1] (1.2×10^{-11} at 90% C.L. [2]).

On the other hand, supersymmetric seesaw mechanism [3] that explains the mysteriously tiny neutrino masses assumes existence of ultra heavy right-handed neutrinos. These heavy particles induce large LFV in charged leptons [4]. Again, the $\mu \to e\gamma$ decays occur near the experimental limit thanks to the large solar neutrino mixing established recently by the SuperKamiokande [5] and the SNO observations [6].

An experiment capable to detect $\mu \to e\gamma$ decays at a branching ratio of 10^{-12} – 10^{-14}, therefore, should be able to explore new physics at extremely high energies, such as grand unification or seesaw mechanism.

2. LFV Search Experiments

Among all the LFV processes involving charged leptons, $\mu \to e\gamma$ and $\mu \to e$ conversion

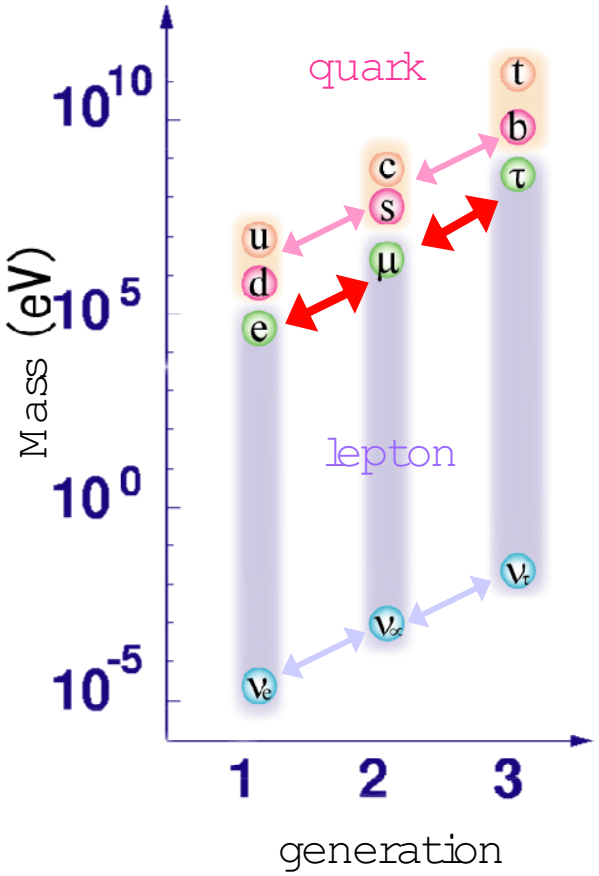

Figure 1: LFV in charged leptons is related by GUTs to the well studied quark mixings and is also implied by the recently established neutrino oscillations via seesaw mechanism.

seem to have highest physics sensitivity in terms of possible experimental reach for generic LFV vertices. In the following major experimental issues concerning searches for these two LFV processes are summarized. A brief comment is also given to another LFV muon decay, $\mu \rightarrow$eee.

2.1. $\mu \rightarrow e\gamma$ *Experiment*

As shown in Fig. 2 (a), a $\mu \rightarrow e\gamma$ event is characterized by the clear 2-body final state. The decay electron and the gamma ray are emitted in opposite directions with the same energy equal to half the muon mass. To utilize this simple kinematics in the search, muons are stopped in a material (a stopping target). Positive muons are used to avoid capture by the target nuclei.

So-called "surface muons" are abundantly produced by bombarding primary protons into a thick production target. The surface muons come from the decays of pions that stop near the surface of the production target and have a sharp momentum spectrum around 29 MeV/c. Because of this narrow momentum spread, they are easily stopped by

a thin target (≈ 100 μm). This is important for achieving good resolutions in measuring positrons and reducing background of annihilation gamma rays. With the naturally 100 % spin polarized surface muons, angular distribution of $\mu \to e\gamma$ can be measured after the discovery. This measurement could pin down the right GUT model.

The major background in a $\mu \to e\gamma$ search is accidental coincidence of a positron, coming from standard Michel decays, and a gamma ray, coming from radiative muon decays or annihilation of positrons. Since the accidental background increases quadratically as the muon rate, a continuous, DC muon beam, that has the lowest instantaneous rate, is best suited for a $\mu \to e\gamma$ search, rather than a pulsed beam. To achieve a sensitivity of 10^{-14} with a detection efficiency $\epsilon \approx 10$ % within one year's time $T \approx 10^7$ sec, a muon rate of $10^{14}/\epsilon/T = 10^{14}/0.1/10^7 \approx 10^8$/sec is necessary.

Requirements on detectors, particularly gamma ray detectors, are very severe. They must have very good resolutions in energy, position and time, both for positrons and gamma rays, to distinguish $\mu \to e\gamma$ from the accidental background. In short, very good detectors are most demanding in a $\mu \to e\gamma$ search.

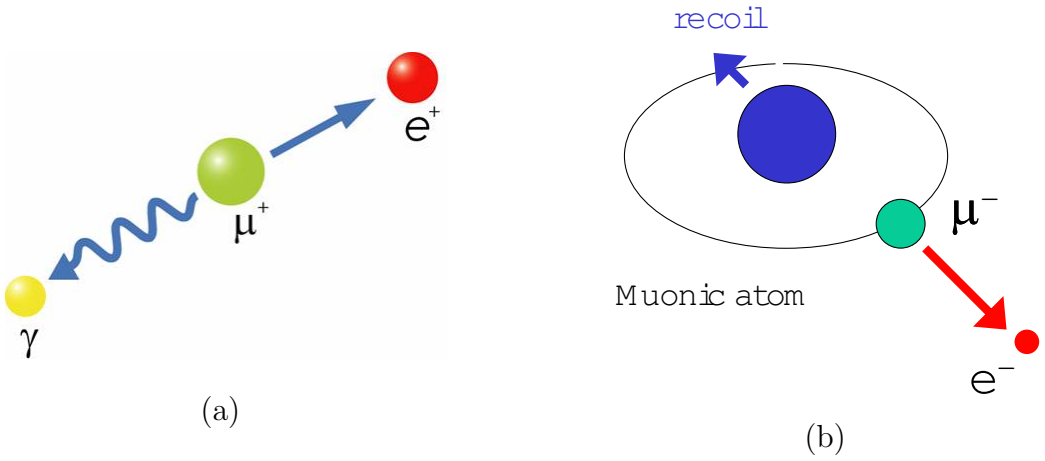

(a) (b)

Figure 2: (a) $\mu^+ \to e^+\gamma$ at rest in a stopping target; (b) $\mu^- \to e^-$ conversion after forming a muonic atom in a stopping target.

2.2. $\mu \to e$ Conversion Experiment

In a $\mu^- \to e^-$ conversion a muon converts into an electron by exchanging a virtual photon (or something more exotic) with the capture nucleus (Fig. 2 (b)). The electron has a monochromatic energy of $E_{\mu\to e} = M_\mu - \delta$, where M_μ is the muon mass and δ is a sum of the binding energy of the muonic atom and the nuclear recoil energy. So the experimental signature is simple: a single monochromatic electron with $E_{\mu\to e}$ (105.1 MeV for Al target). Negative muons must be used to form muonic atoms with the target nuclei.

For generic photonic LFV vertices, physics sensitivity of $\mu \to e$ conversion is two orders of magnitude lower than $\mu \to e\gamma$: ($\mu \to e$ conversion)/($\mu \to e\gamma$) = 1/390 for Al target, 1/249 for Ti, and 1/340 for Pb in terms of branching ratios. Thus, a $\mu \to e\gamma$ branching ratio of 1×10^{-14} corresponds to 3×10^{-17} for $\mu \to e$ conversion. To achieve

this sensitivity, a negative muon beam of an intensity of 10^{10} - 10^{11}/sec is necessary.

Getting such a high muon rate is a big issue. Because there is no "surface muon beam" for negative muons, such a high intensity beam tends to have a much broader spectrum and is usually contaminated by various other particles, particularly pions.

Major backgrounds in a $\mu \rightarrow$ e conversion search are (a) electrons from muon decays in orbit and (b) beam-related background.

The energy E_e of the "decay in orbit" electron has a spectrum falling off rapidly as $(E_{\mu\rightarrow \mathrm{e}} - E_e)^5$. By improving the electron energy resolution σ_{E_e}, this background decreases as $\sigma^5_{E_e}$. Since the energy resolution is dominated by energy loss in the stopping target, a thinner target is required. However, stopping efficiently a broad spectrum of muons in a thin target is quite difficult.

There are various beam-related background caused by beam contaminants such as pions. For example, pions may be radiatively captured by the target nuclei, emitting gamma rays which subsequently convert into electrons. Thus, in short, a very good muon beam is most demanding in a $\mu \rightarrow$ e conversion search.

A few comments on a $\mu \rightarrow$eee process follow. Physics sensitivity of $\mu \rightarrow$eee is two orders of magnitude lower than $\mu \rightarrow \mathrm{e}\gamma$: $(\mu \rightarrow \mathrm{eee})/(\mu \rightarrow \mathrm{e}\gamma) = 1/170$. Since overlapping events dominate background, a DC muon beam is required; then, with the currently available muon facilities, only a similar branching ratio as $\mu \rightarrow \mathrm{e}\gamma$ may be achieved. This is not competitive to the $\mu \rightarrow \mathrm{e}\gamma$ and $\mu \rightarrow$ e conversion experiments. Note that the experimental setup would be very different from that of $\mu \rightarrow \mathrm{e}\gamma$.

3. The MEG Experiment

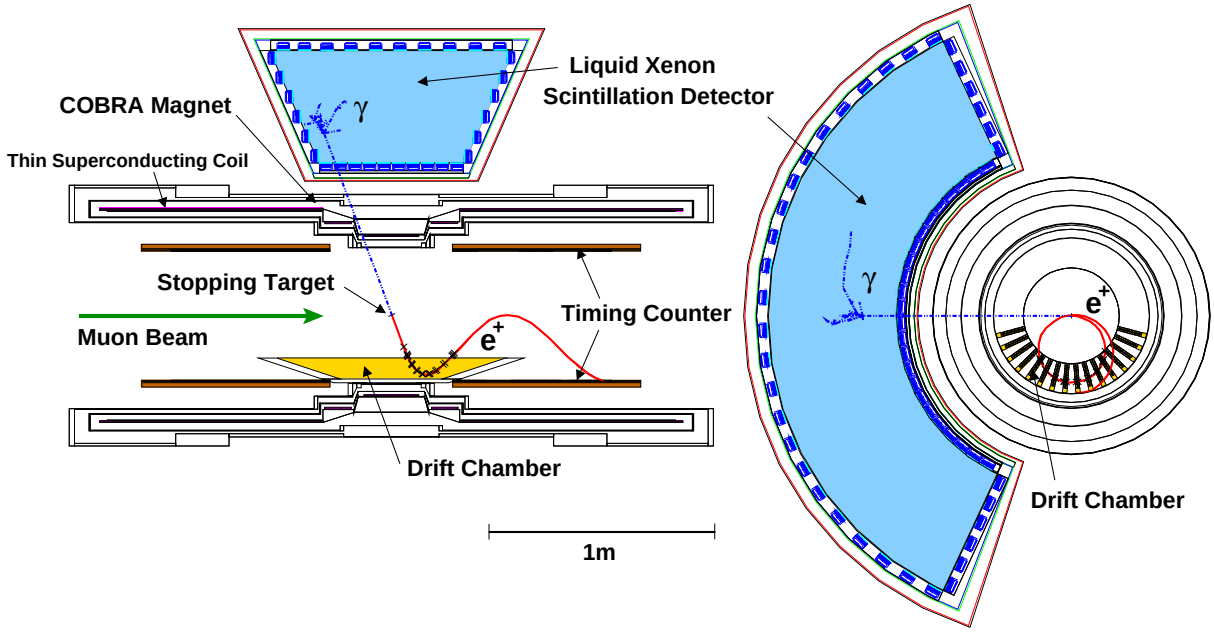

Figure 3: A schematic experimental setup of the MEG experiment.

In 1999 a new proposal to search for $\mu \rightarrow e\gamma$ decays by Japanese physicists was approved by the Paul Scherrer Institute (PSI), Switzerland [7]. The experimental collaboration has since evolved to approximately 50 physicists from Japan, Switzerland, Italy and Russia and is now called the MEG (Muon to Electron and Gamma) collaboration. It is now scheduled to start physics runs in 2006 with an initial sensitivity of 10^{-13}, eventually down to 10^{-14}. Detector components are currently being constructed and will be assembled and tested toward the end of 2005. The experiment is capable to measure angular distribution of $\mu \rightarrow e\gamma$ upon discovery [8], thanks to fully polarized surface muon beam.

The experimental set-up is schematically shown in Fig. 3. DC surface muon beam of 10^{7-8}/sec is focused and stopped in a thin plastic target. Gamma rays from $\mu \rightarrow e\gamma$ decays are measured by liquid xenon scintillation detector located just outside a very thin solenoidal magnet called COBRA. Positrons are tracked by low material drift chambers inside COBRA which provides specially graded magnetic field. Their timings are measured by plastic scintillation counters in the second turn of their trajectories.

The unprecedented sensitivity of the MEG experiment has been made possible by the following three key components:

- highest intensity DC surface muon beam available at PSI,
- special positron spectrometer with graded magnetic field, and
- liquid xenon scintillation gamma ray detector.

These key components are described in some more detail in the following sections.

3.1. Intense DC Muon Beam at PSI

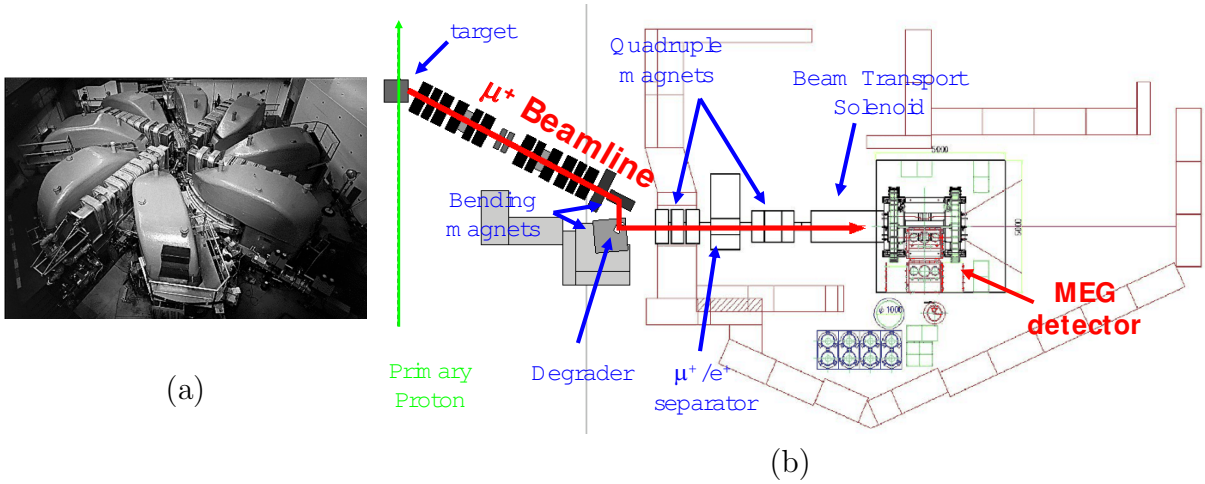

Figure 4: (a) The 590 MeV proton cyclotron at PSI constantly provides a beam current exceeding 1.8 mA. (b) The πE5 beamline for the MEG experiment.

The 590MeV proton cyclotron at PSI (Fig. 4 (a)), constantly operating with a beam current exceeding 1.8mA with a total beam power of more than 1 MW, is able to produce

the highest intensity DC muon beam in the world. This is the best and only place suitable for a $\mu \to e\gamma$ experiment.

The final setup of the πE5 beamline for the MEG experiment is shown in Fig. 4 (b). Added downstream of the existing beamline are two sets of quadrupole magnets and a solenoidal magnet to transport and focus the beam onto a small target (a few cmϕ). A DC separator is placed to reject unwanted positrons in the beam.

Beamline commissioning started in the spring of 2004. A preliminary beam tuning demonstrated that a muon stopping rate of 10^8/sec, i.e. more than 10^{15} stopped muons per year, is reasonably expected.

The final beam tuning for physics runs will start in the summer of 2005 just after a delivery of the beam transport solenoid.

3.2. COBRA Positron Spectrometer Magnet

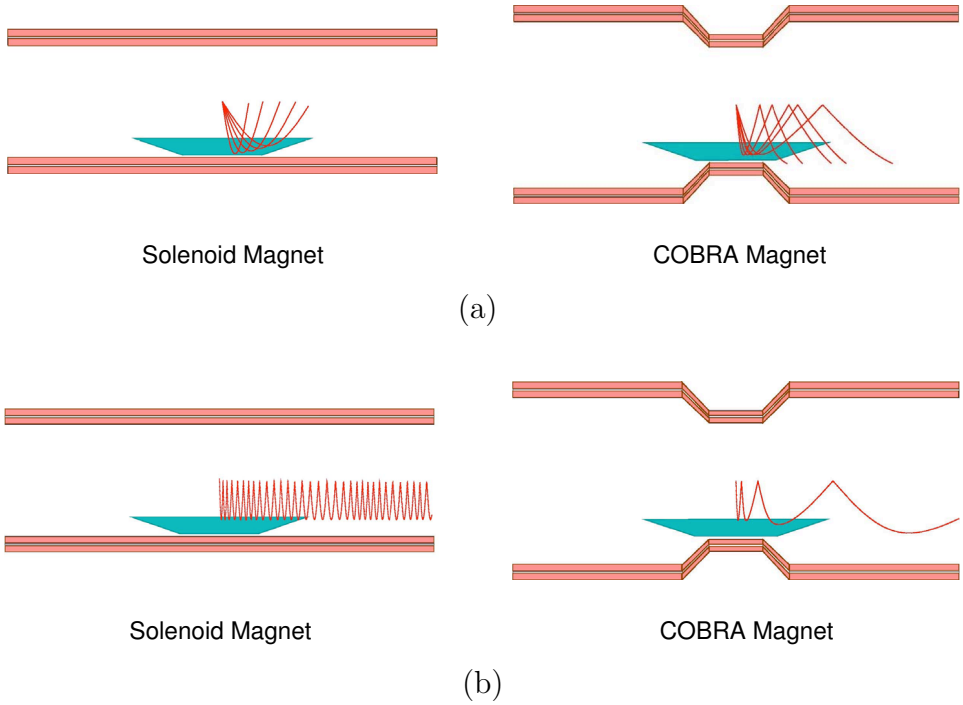

Figure 5: A special graded magnetic field of COBRA has two advantages over a normal solenoid: (a) Positrons with the same momentum travel with the same bending radius; (b) Positrons are quickly swept away from the tracking volume.

The COBRA (COnstant Bending RAdius) positron spectrometer consists of a superconducting solenoidal magnet designed to form a special graded magnetic field (1.27 T at the center and 0.49 T at the both ends), in which positrons with the same absolute momenta follow trajectories with a constant projected bending radius, independent of the emission angles over a wide angular range, as shown schematically in Fig. 5 (a). This allows to sharply discriminate high momentum signal positrons ($p = m_\mu/2 = 52.8\mathrm{MeV}/c$) out of 10^8 Michel positrons emitted every second from the target. Only high momentum

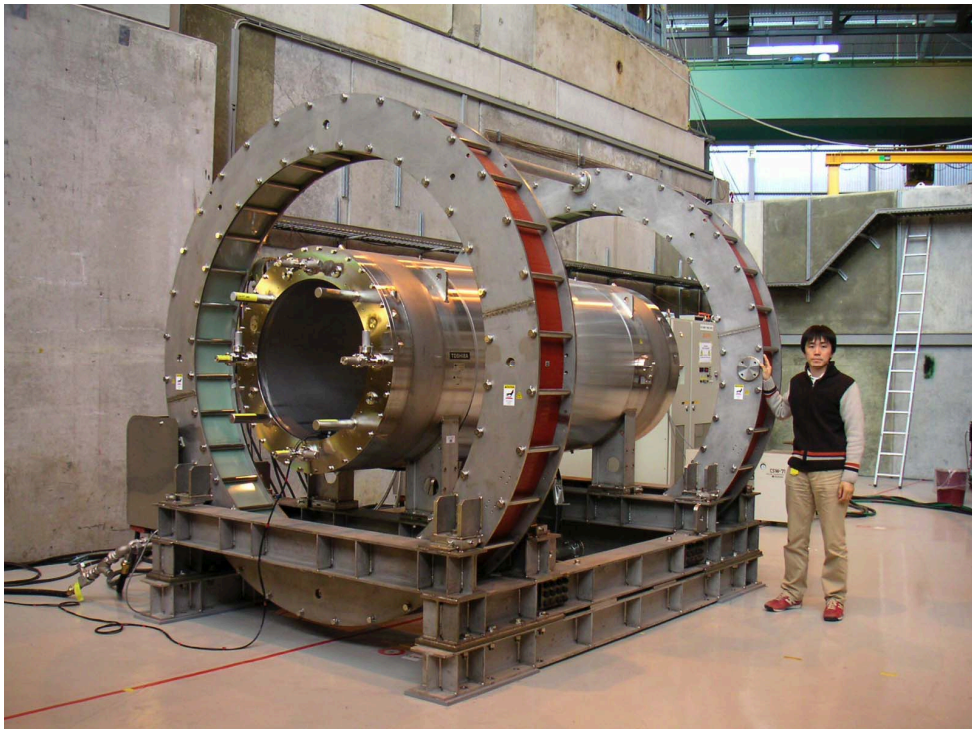

Figure 6: The COBRA magnet at the πE5 beamline. Two large coils around the main magnet are to compensate and suppress the magnetic field at the LXe detector.

positrons enter the drift chamber volumes. The graded field also helps to sweep away curling tracks quickly out of the tracking volume (Fig. 5 (b)), thereby reducing accidental pile-up of the Michel positrons.

High strength Al stabilized conductor is used to make the magnet as thin as $0.197X_0$, so that 85% of 52.8MeV/c gamma rays traverse the magnet without any interaction before entering the gamma ray detector placed outside the magnet. A He-free, simple and easy operation of the magnet is realized with a GM refrigerator.

As the COBRA magnet does not have a return yoke, a pair of compensation coils (seen as two large rings in Fig. 6) suppress the stray magnetic field below 50 Gauss in the vicinity of the gamma ray detector, so that the photomultiplier tubes can operate.

The COBRA magnet was constructed in Japan and was then transported and installed at the πE5 beamline. Various tests including full excitation and quenching were all successful. Preliminary mapping of the field shows a beautifully graded magnetic field just as designed and successful field suppression at the gamma ray detector position. It now operates routinely at the beamline (Fig. 6).

3.3. Liquid Xenon Gamma Ray Detector

An innovative liquid xenon (LXe) scintillation detector was specially devised for this experiment to make very precise measurements of energy, position and timing of gamma rays. The detector holds an active LXe volume of 800 ℓ. Scintillation light emitted inside

LXe are viewed from all sides by approximately 850 photomultiplier tubes (PMTs) that are immersed in LXe in order to maximize direct light collection. The detector utilizes only scintillation light without any attempt to measure ionization.

High light yield of LXe (roughly 75% of NaI) and its uniformity are necessary ingredients for good energy resolution. A scintillation pulse from xenon is very fast and has a short tail, thereby minimizing the pile-up problem. Distributions of the PMT outputs enable a measurement of the incident position of the gamma ray with a few mm accuracy. The position of the conversion point is also estimated with an accuracy that corresponds to a timing resolution of about 50 psec.

A major ambiguity of this newly developed detector was absorption of the UV scintillation light ($\lambda = 178$ nm) inside LXe. LXe itself should in principle be transparent to its own scintillation light thanks to the scintillation mechanism through the excimer state Xe_2^*. However, possible impurities in LXe, such as water and oxygen at ppm level, considerably absorb scintillation light and could possibly degrade the detector performance.

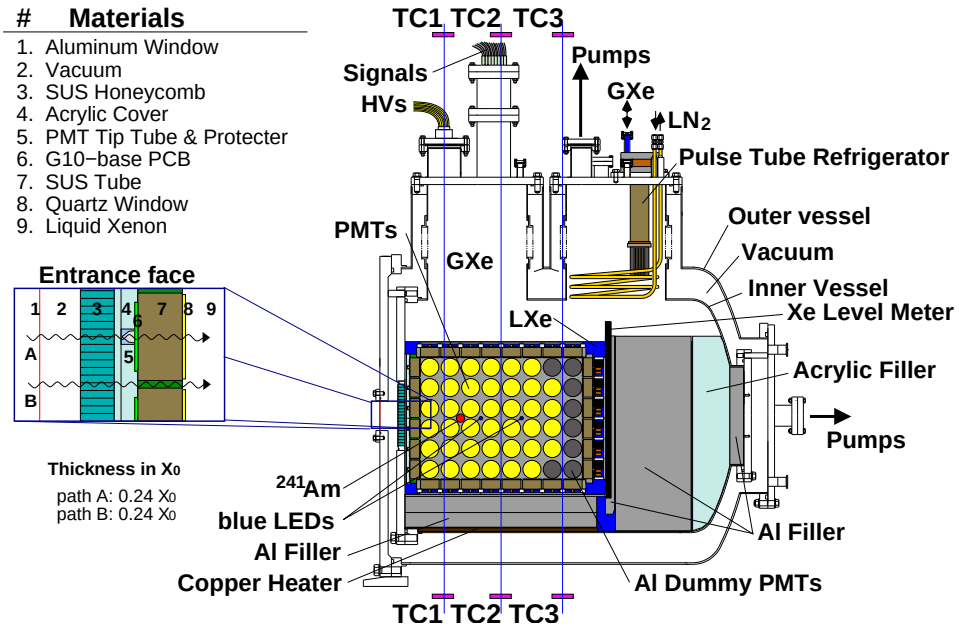

(a)

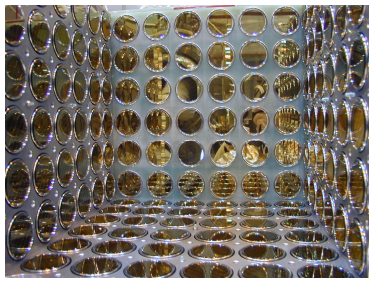

(b)

Figure 7: (a) A schematic view of 100 ℓ prototype detector. (b) Inside the detector: PMTs are looking into the LXe volume.

3.3.1. Prototype Detector

A 100 ℓ prototype detector with an active volume of $372 \times 372 \times 496$ mm^3 (69 ℓ) surrounded by 228 PMTs was built (Fig. 7) in order to gain practical experiences in operating such a new device and to prove its excellent performance. Xenon must be kept at its liquid phase temperature of approximately -110 °C during operation. The cryostat consists of thermal insulated vessels equipped with a pulse tube refrigerator developed at KEK. To minimize gamma ray interactions before the active region of the detector, a thin aluminum plate and a honeycomb window made of stainless steel are used as an entrance window. Including the PMTs and their holders, the front materials amount to a total thickness of 0.24 X_0, as summarized in Fig. 7 (a). Taken from inside the detector, a photograph of Fig. 7 (b) shows how the PMTs are aligned inside.

PMTs that operate at the LXe temperature and stand up to 0.3 MPa pressure were developed in cooperation with Hamamatsu Photonics K.K. Since standard photocathode materials become inefficient at such low temperatures due to increasing resistivity, aluminum strips are coated on the window to reduce the resistivity. A synthetic quartz window is used to allow for the UV scintillation light. The short axial length of 32 mm is realized by adoption of metal channel dynode structure. With this structure the PMTs can sustain up to 50 Gauss of magnetic field.

After evacuation and pre-cooling of the vessel, xenon is liquefied by using liquid nitrogen and the refrigerator. Gas xenon flows through a gas purifier and molecular filters before entering the vessel. After liquefaction, LXe is maintained at 168 K and 0.13 MPa by the refrigerator. The detector was kept in stable operation continuously and successfully for more than 2000 hours for the measurement described below.

3.3.2. Scintillation Absorption in LXe

After calibrating PMT gains by blue LEDs, cosmic rays and ^{241}Am alpha sources placed inside the detector were measured. These measurements indicated a strong absorption of scintillation light as shown by the open data points in Fig. 8 (a). Distant PMTs saw much less light from the alpha sources than closer ones. Although xenon was well purified before filling the detector vessel, some inner components of the prototype are made of G10 and acrylic that are known to absorb and desorb water. According to subsequent systematic studies on the residual gas by means of mass spectroscopy and build-up tests, the main impurity was water at the level of ppm.

To remove the water contamination, a system to circulate and purify xenon was installed to the detector (Fig. 8 (b)). Light absorption was monitored with cosmic rays and the alpha sources. After one month circulation, light absorption length improved from 12 cm to longer than 100 cm (the closed data points in Fig. 8 (a)). With the achieved absorption length of 100 cm, Monte Carlo simulation predicts an energy resolution of

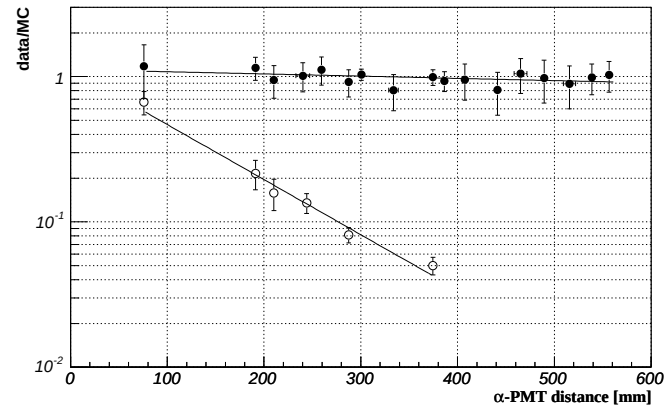

(a)

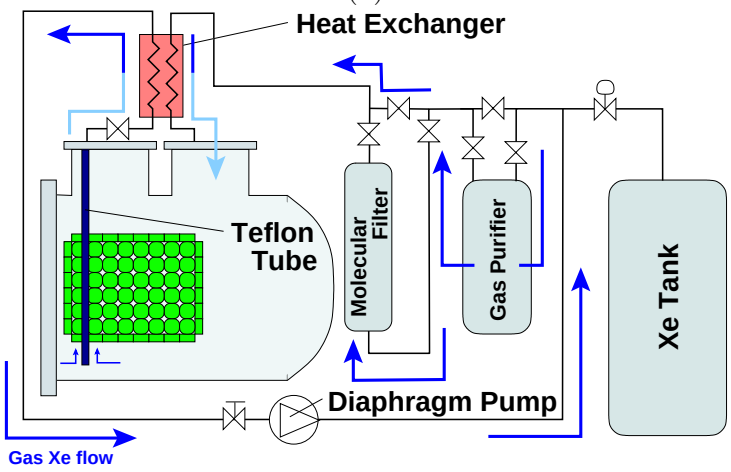

(b)

Figure 8: (a) PMT outputs normalized to MC simulation without absorption are plotted as a function of the source–PMT distance at the beginning (open circles) and after purification (closed circles). The solid lines are fitted results. (b) The circulation and purification system of xenon.

about 1.2 % for 52.8 MeV gamma rays, quite adequate for the MEG experiment.

3.3.3. Detector Performance

To verify the performance of the LXe detector it was irradiated by gamma rays with known energies of 10 – 129 MeV, either from laser Compton back-scatterings, or from π^0 decays in the charge exchange reactions, $\pi^- p \rightarrow \pi^0 n$.

Gamma rays with upper edge energies of 10, 20 and 40 MeV are available from the laser–electron Compton back-scattering at the TERAS electron storage ring at the National Institute of Advanced Industrial Science and Technology (AIST), Tsukuba, Japan (Fig. 9 (a)). An example of the laser Compton gamma ray spectra measured by the detector is shown in Fig. 9 (b). Smearing of the Compton edge indicates the detector resolution.

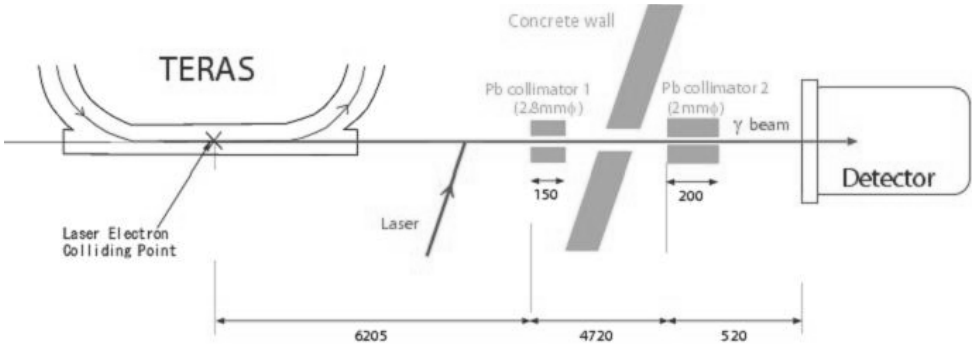

(a)

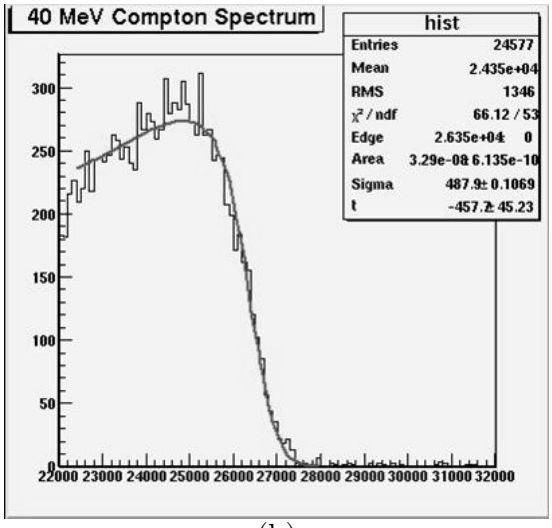

(b)

Figure 9: (a) Laser-electron Compton back-scattering facility at the TERAS storage ring at the AIST, Tsukuba. (b) Measured Compton spectrum for Compton edge energy of 40 MeV.

Transporting the detector to the Paul Scherrer Institute, Switzerland, π^0 decays in the charge exchange reactions, $\pi^- + p \to \pi^0 + n$, were used to obtain monochromatic gamma rays of 55 and 83 MeV by tagging coincident gamma rays in the opposite directions. Another reaction, $\pi^- + p \to n + \gamma$, also provided monochromatic 129 MeV gamma rays. An example of 55 MeV gamma ray spectrum is shown in Fig. 10 (a). The lower tail of the spectrum is caused by shower leakage from the front side of the detector and interactions in the material in front of liquid xenon. This tail only affects the detection efficiency. It is the upper side resolution that really discriminates the background, thus determines the sensitivity for $\mu \to e\gamma$ events.

Preliminary energy resolutions obtained from these measurements are summarized in Fig. 10 (b). The resolution scales according to $1/\sqrt{E}$ just as indicated by a straight line in the figure. For 52.8 MeV gamma rays from $\mu \to e\gamma$ decays, the energy resolution is $\sim$1.4% in σ. These measurements also provided position resolutions that vary from 2 mm to 3.5 mm, depending on incident positions of gamma rays, and timing resolutions

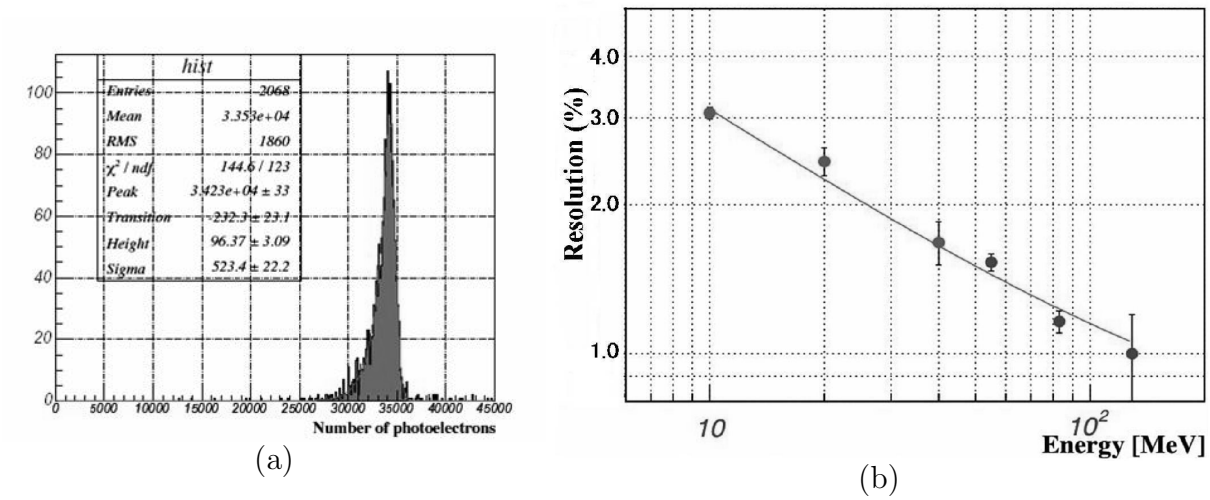

(a) (b)

Figure 10: (a) A measured spectrum for a monochromatic 55 MeV gamma rays from $\pi^- p \to \pi^0 n$. (b) Obtained energy resolutions as a function of gamma ray energies (preliminary).

of about 100 psec. All together, the detector satisfies necessary resolutions to reach the initial goal of sensitivity of 10^{-13}.

3.3.4. Prospects

To further improve the detector performance, new types of PMTs have been recently developed. A preliminary measurement indicated quantum efficiency improved by a factor of about 3 over the present PMTs used in the prototype detector. To see how this improvement will be translated into the detector performance and the experimental sensitivity, we are planning to carry out another beam test using these new PMTs. In this beam test, trigger modules and new waveform digitizers for the final experiment will be also tested.

The cryostat vessel of the LXe detector for the MEG experiment is currently under construction and will be delivered to PSI next year. New PMTs are arriving and will be calibrated by next summer. Then towards the end of 2005 everything will be assembled and tested to get ready for physics runs planned in 2006.

4. The MECO Experiment

The MECO (Muon Electron COnversion) experiment [9] was proposed to search for $\mu \to$ e conversion at a sensitivity below 10^{-16}. For $\mu \to$ e conversion events occurring at 1×10^{-16}, 5 signal events may be detected with 0.5 background events in one year running. It was scientifically approved in 1997 by Brookhaven National Laboratory.[a]

Its schematic layout is shown in Fig. 11. It consists of three graded-field superconducting solenoids: a production solenoid to collect pions produced at the production target,

[a]Its construction was recently approved for the fiscal year of 2005. It will take at least 5 years for construction.

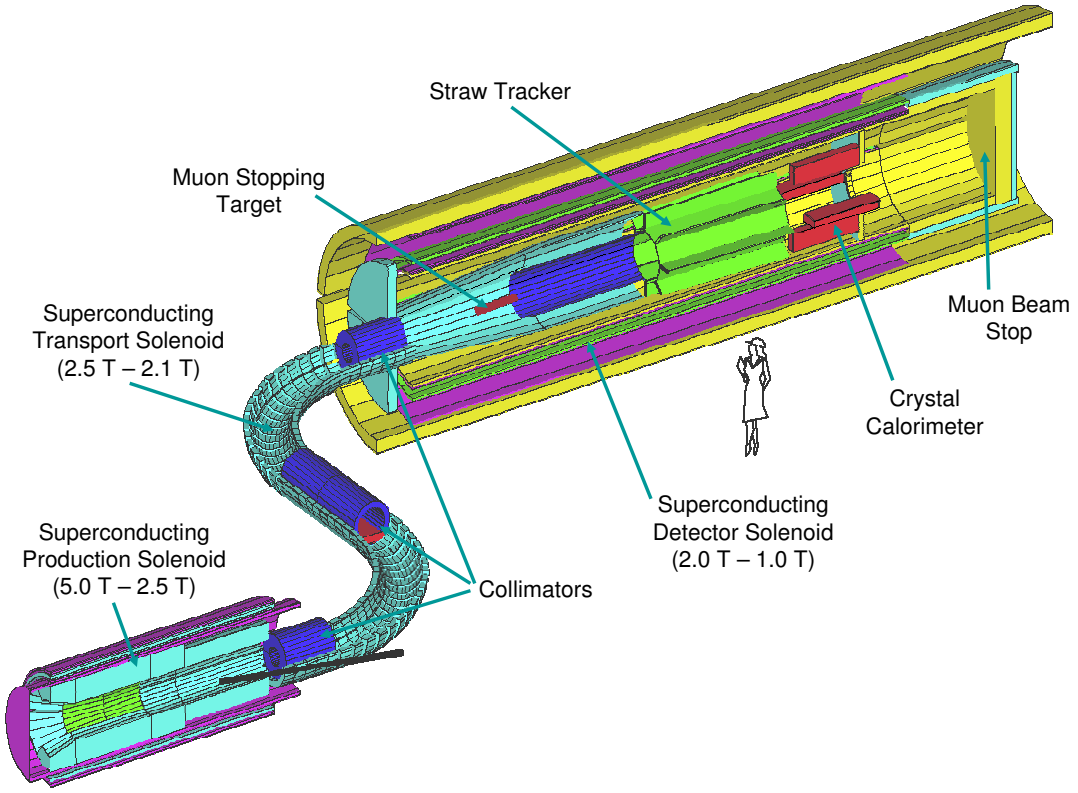

Figure 11: A schematic layout of the MECO experiment.

a curved transport solenoid to capture muons from pion decays and select low momenta and negative charges by means of collimators, and a spectrometer solenoid for measuring signal electrons.

The use of a graded-field solenoid to collect pions leads to a 1000 fold increase in muon intensity (to 10^{11}/sec) over the previous experiment. This idea was originally proposed for a Russian experiment [10].

A 30 nsec pulsed proton beam is extracted every 1.35 μsec during a 0.5 sec beam spill from the Alternating Gradient Synchrotron (AGS) as shown in Fig. 12. To avoid beam-related background, the MECO experiment only operates 0.6 μsec after the beam pulse, when all the backgrounds have fallen off.

To stop a broad spectrum of muons, 17 layers of 0.2 mm thick Al targets are used. Aluminum is chosen as target material, because its muon capture lifetime (0.9 μsec) matches the measurement cycle while heavier elements have much shorter lifetimes.

5. The PRISM/PRIME project

PRISM (Phase-Rotated Intense Slow Muons) [11] is an ambitious project to produce high intensity muon beam with narrow energy spread and less contamination, proposed to be built at the J-Parc 50 GeV proton ring, currently under construction at Tokai, Japan. Its schematic layout is shown in Fig. 13. A Fixed-Field Alternating Gradient

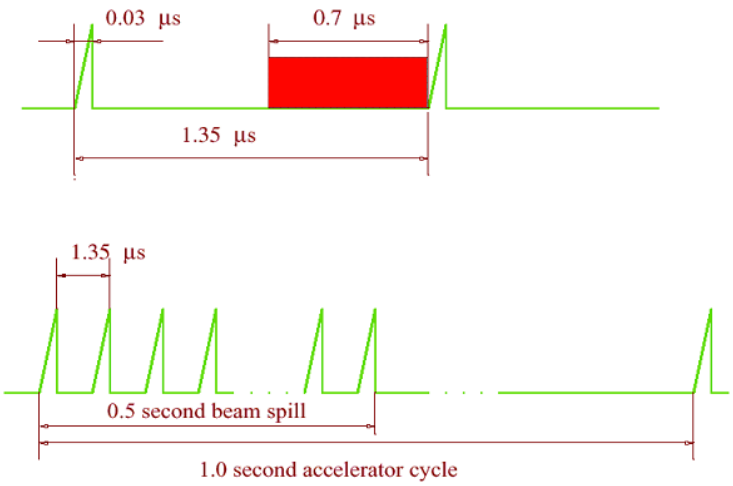

Figure 12: Pulse structure of proton beam for the MECO experiment at the AGS ring, BNL. Only the last 0.7 μs out of the 1.35 μs cycle is used for measurement. Note that effective lifetime of negative muons in Al target is 0.9 μs.

synchrotron (FFAG) is used to carry out "phase rotation," i.e. a conversion of an original short pulse beam with wide momentum spread ($\pm$30 %) into a long pulse beam with narrow momentum spread ($\pm$3 %) by strong RF field. After 5 turns in the FFAG ring for the phase rotation, pions in the beam all decay out. Given 10^{14} protons /sec from the J-Parc ring, the PRISM facility should be able to provide 10^{11} - 10^{12} muons/sec.

There are still several R&D items to study: for example, low energy pion production and capture system, and injection/extraction of muons into/from the FFAG ring. A real-size FFAG ring, which may be used for PRISM later, is being constructed at Osaka University for R&D studies.

PRIME (PRISM Mu E) [11] is a proposed experiment to search for $\mu \rightarrow$ e conversion at the future PRISM facility. Because of a very low duty factor of the PRISM beam, the experiment has to handle an extremely high instantaneous rate of 10^{10} - 10^{11} muons per beam bunch. In the PRIME experiment a curved solenoid spectrometer is used to transport only electrons with desired momenta from the stopping target to the detector. Thanks to PRISM's good quality muon beam, with a higher efficiency and a better momentum resolution, a sensitivity of the level of 10^{-18} may be expected.

6. Conclusion

Expectations for LFV search experiments are now higher than ever, with the observed large neutrino mixings, and also with successful supersymmetric grand unification theories. First of all the coming LFV experiments, the MEG experiment, expected to start in 2006, has a good chance to make the first discovery of new physics before the LHC. Its capability to measure the angular distribution of $\mu \rightarrow e\gamma$ events, together with possible discoveries by the LHC experiments and the $\mu \rightarrow$ e experiments, could eventually pin

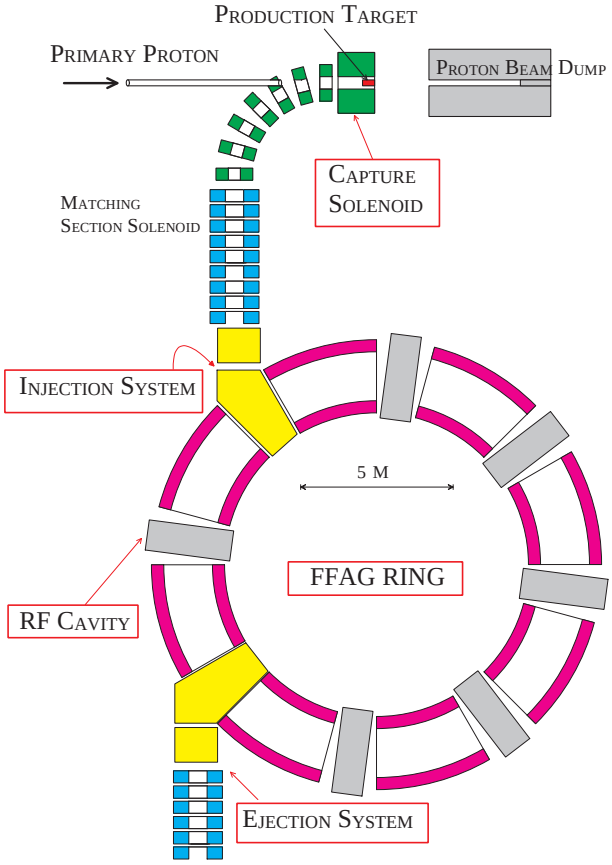

Figure 13: A schematic layout of PRISM (not scaled).

down a new physics scenario up to an extremely high energy.

7. References

[1] R. Barbieri and L.J. Hall, Phys. Lett. **B338** (1994) 212; R. Barbieri, L.J. Hall, and A. Strumia, Nucl. Phys. **B445** (1995) 219.

[2] MEGA Collaboration, M.L. Brooks *et al.*, Phys. Rev. Lett. **83** (1999) 1521.

[3] M. Gell-mann, P. Ramond and R. Slansky, in Supergravity, Proceedings of the Workshop, Stony Brook, New York, 1979, ed. by P. van Nieuwenhuizen and D.Freedman (North-Holland, Amsterdam); T. Yanagida, in Proceedings of the Workshop on Unified Theories and Baryon Number in the Universe, Tsukuba, Japan, edited by A. Sawada and A.Sugamoto (KEK Report No. 79-18, Tsukuba) (1979).

[4] J. Hisano and D. Nomura, Phys. Rev. **D59** (1999) 116005 and references therein.

[5] Super-Kamiokande Collaboration, Phys. Rev. **D69** (2004) 011104; Super-Kamiokande Collaboration, Phys. Lett. **B539** (2002) 179-187.

[6] SNO Collaboration, Q.R. Ahmad *et al.*, Phys. Rev. Lett. **87** (2001) 071301; Phys. Rev. Lett. **89** (2002) 011301; Phys. Rev. Lett. **89** (2002) 011302; Phys. Rev.

Lett. **92** (2004) 181301.
[7] T. Mori *et al.*, Research Proposal to PSI, R-99-5, May 1999; A. Baldini *et al.*, Research Proposal to INFN, Sep. 2002. These documents and the updated information of the MEG experiment are available at `http://meg.web.psi.ch/docs/`.
[8] S. Yamada, "$\mu \to e\gamma$ decay angular measurement by the MEG experiment," in this Proceedings.
[9] The proposal and the updated information of the MECO experiment are available at `http://meco.ps.uci.edu/`.
[10] R.M. Djilkibaev and V.M. Lobashev, Sov. J. Nucl. Phys. **49**(2), (1989) 384; "MELC Experiment to Search for the $\mu^- A \to e^- A$ Process," V.S. Abadjev, *et al.*, INR preprint 786/92, November 1992.
[11] Letters of Intent for PRISM and PRIME are available at `http://www-ps.kek.jp/jhf-np/LOIlist/LOIlist.html`.